Collapse of a ring polymer: Comparison of Monte Carlo and Born–Green–Yvon integral equation results

Mark P. Taylor, James L. Mar, and J. E. G. Lipson
Department of Chemistry, Dartmouth College, Hanover, New Hampshire 03755

(Received 20 November 1996; accepted 17 December 1996)

The equilibrium properties of an isolated ring polymer are studied using a Born–Green–Yvon (BGY) integral equation and Monte Carlo simulation. The model polymer is composed of n identical spherical interaction sites connected by universal joints of bond length σ. In particular, we study rings composed of up to $n=400$ square-well spheres with hard-core diameter σ and well diameter $\lambda\sigma$ $(1\leqslant\lambda\leqslant 2)$. Intramolecular site–site distribution functions and the resulting configurational and energetic properties are computed over a wide range of temperatures for the case of $\lambda=1.5$. In the high temperature (good solvent) limit this model is identical to a tangent-hard-sphere ring. With decreasing temperature (worsening solvent) both the radius of gyration and the internal energy of the ring polymer decrease, and a collapse transition is signaled by a peak in the single ring specific heat. In comparison with the Monte Carlo calculations, the BGY theory yields quantitative to semiquantitative results for $T\gtrsim T_\theta$ and is qualitatively accurate for $T\lesssim T_\theta$, where T_θ is the theta temperature. The thermal behavior of an isolated square-well ring is found to be quite similar to the behavior of an isolated square-well chain. The BGY theory indicates that rings and chains have comparable theta and collapse transition temperatures. In the low temperature limit (collapsed state) the microscopic structure of rings and chains becomes nearly identical. © *1997 American Institute of Physics.* [S0021-9606(97)50312-6]

I. INTRODUCTION

Polymers in dilute solution undergo a transition from an expanded to a collapsed state when solvent conditions are changed from ''good'' to ''poor.''[1,2] This collapse or coil–globule transition has been the subject of numerous theoretical[3–13] and experimental[14–22] investigations. Although most of these studies have considered linear chain polymers, a collapse transition is also expected for polymers of more complex molecular architecture. Indeed, recent lattice and continuum simulation studies have shown that ring polymers undergo a collapse transition very similar to that of chains.[5,9,13]

A polymer molecule of any specified architecture or topology can be modeled as a collection of simple fluid monomers subject to a set of specific bonding constraints. The intramolecular structure of such an interaction-site polymer can be described in terms of a set of site–site distribution functions analogous to the pair distribution function of a simple fluid. In principle these site–site distribution functions can be calculated via the integral equation techniques of liquid state theory.[23–27] In this approach the site–site potential between nonbonded monomers is assumed to represent an effective potential which implicitly includes the effects of a continuum solvent. Thus, high and low temperatures correspond to good and poor solvent conditions, respectively.

We have recently developed a Born–Green–Yvon (BGY) integral equation theory for an isolated interaction-site linear chain polymer and used this theory to study the chain collapse transition.[27] Here we extend the BGY approach to the case of an isolated interaction-site ring polymer and study the analogous ring collapse transition. In particular we consider polymers formed from square-well-sphere monomers. In order to test the BGY theory we have also performed Monte Carlo simulations on isolated square-well ring (and linear chain) polymers. The equilibrium properties computed in this study include an average site–site density distribution, mean-square radius of gyration, average internal energy, and specific heat. The BGY results for all of these quantities are in near quantitative agreement with the simulation data in the high temperature (good solvent) regime. In the low temperature (poor solvent) regime qualitative agreement between theory and simulation is obtained. The BGY results indicate that rings and chains have very similar theta and collapse transition temperatures.

II. THEORY

A. Ring distribution functions

In this work we study an isolated ring polymer molecule which is constructed from n identical simple fluid monomers. These monomers, or interaction sites, are connected by universal joints of bond length σ and interact via a spherically symmetric site–site potential $u_{ij}(r)$, where r is the distance between nonbonded sites i and j (i.e., $1<|i-j|<n-1$). The n-mer ring can be viewed as a linear n-mer chain in which the end sites (i.e., ''1'' and ''n'') are bonded. The microscopic structure of such an interaction-site molecule can be described in terms of a set of site–site intramolecular distribution functions $w_{ij}(r)$ which are proportional to the probability that two sites i and j are separated by a distance r.[27] For a ring polymer these distribution functions are trans-

lationally invariant with respect to the labeling of the sites. In other words, labeling one of the n identical sites as site ''1,'' the following two equalities are true:

$$w_{ij}^{\mathrm{ring}}(r)=w_{1,|i-j|+1}^{\mathrm{ring}}(r), \tag{1a}$$

$$w_{1\nu}^{\mathrm{ring}}(r)=w_{1,n-\nu+2}^{\mathrm{ring}}(r). \tag{1b}$$

Thus for an n-mer ring there are actually only $n/2$ unique site–site distribution functions. Due to the constraints of chain connectivity the $w_{1\nu}^{\mathrm{ring}}(r)$ distribution function is identically zero for $r/\sigma>\min(\nu-1,n-\nu+1)$.

As noted above, the set of all possible configurations of an n-mer ring (which includes those containing knots) is given by the subset of all possible configurations of an n-mer chain in which the terminal sites of the chain are in contact (i.e., $r_{1n}=\sigma$). Thus, the intramolecular site–site distribution functions for an n-mer ring can be expressed exactly in terms of the three-site n-mer chain distribution functions as follows:

$$w_{1\nu}^{\mathrm{ring}}(r_{1\nu})=\frac{4\pi\sigma^3 Z_n^{\mathrm{chain}}}{Z_n^{\mathrm{ring}}} \times\int d\mathbf{r}_n w_{1\nu n}^{\mathrm{chain}}(r_{1\nu},r_{\nu n},r_{1n})s_{1n}(r_{1n}), \quad 1<\nu<n, \tag{2}$$

where $s(r)=\delta(r-\sigma)/4\pi\sigma^2$ is the intramolecular distribution function between bonded sites and Z_n^{chain} and Z_n^{ring} are the partition functions for an isolated n-mer chain and ring, respectively. The two-site ring distribution functions obey the normalization

$$\int dr 4\pi r^2 w_{1\nu}^{\mathrm{ring}}(r)=1 \tag{3}$$

and the ratio $Z_n^{\mathrm{ring}}/Z_n^{\mathrm{chain}}$ is equal to the probability that an n-mer chain will be found in a closed ring configuration [i.e., $4\pi\sigma^3 w_{1n}^{\mathrm{chain}}(\sigma)$]. Since the ring distribution functions are translationally invariant, the above equation is sufficient to compute the complete set of n-mer ring two-site distribution functions [noting that $w_{1n}^{\mathrm{ring}}(r)=s(r)$]. In the special case of a tangent-hard-sphere 4-mer chain the three-site distribution function can be computed exactly and thus, using Eq. (2), the tangent-hard-sphere 4-mer ring site–site distribution function can also be determined exactly (see the Appendix). In general, however, three-site distribution functions for chains are not easily obtained and one must resort to approximate methods.

In a recent work we derived a Born–Green–Yvon (BGY) integral equation for the site–site distribution functions of an isolated interaction-site chain.[27] The single chain BGY equation also involves a three-site distribution function which we expressed in terms of two-site functions using a superpositionlike approximation. Results from this BGY theory compared quite well with the available Monte Carlo results for isolated hard-sphere and square-well chains. The same superposition approximation can be used in the expression for the ring distribution functions [Eq. (2)] and, using our single chain BGY results, one can construct a self-contained theory for the isolated interaction-site ring. The superpositionlike approximation is given by

$$w_{1\nu n}^{\mathrm{chain}}(r_{1\nu},r_{\nu n},r_{1n})=w_{1\nu}^{\mathrm{chain}}(r_{1\nu})w_{\nu n}^{\mathrm{chain}}(r_{\nu n})\Gamma_{1(\nu)n}(r_{1n}), \tag{4}$$

where $\Gamma_{1(v)n}(r_{1n})$ depends on two-site distribution functions. The exact functional form of $\Gamma_{1(v)n}$ is not important here since Eq. (2) requires only the $r_{1n}=\sigma$ limit [in which case $\Gamma_{1(v)n}$ is a constant and Eq. (4) is equivalent to a Markov approximation[28]]. Substituting this superposition approximation into the exact expression for the two-site n-mer ring distribution function [Eq. (2)] leads to the following general expression:

$$w_{1\nu}^{\mathrm{ring}}(r)=\frac{1}{N_{1\nu}}\frac{w_{1\nu}^{\mathrm{chain}}(r)}{r}\int_{r-\sigma}^{r+\sigma}dt t w_{\nu n}^{\mathrm{chain}}(t), \tag{5}$$

where N_{1v} is a normalization constant. This simple equation allows one to compute the site–site distribution functions of an n-mer ring molecule given the distribution functions of the corresponding n-mer chain. Although other approaches are possible, here we use our single chain BGY equation [Eq. (13) of Ref. 27] to compute the required chain distribution functions. This results in a self-contained BGY theory for the isolated interaction-site ring molecule.

Since Eq. (5) is not exact, the second translational invariance condition given above [Eq. (1b)] is not guaranteed. Just how well this condition is satisfied provides a measure of the internal consistency of the theory and of the accuracy of the Eq. (4) superposition approximation. In practice, it is best to compute both $w_{1v}^{\mathrm{ring}}(r)$ and $w_{1,n-v+2}^{\mathrm{ring}}$ and then average these pairs of functions.

The above set of results is valid for an arbitrary site–site potential. However in the following we restrict ourselves to the square-well sphere potential:

$$\beta u(r)=\begin{cases}\infty & r<\sigma\\ -\beta\epsilon & \sigma<r<\lambda\sigma\\ 0 & r>\lambda\sigma,\end{cases} \tag{6}$$

where $\beta=1/k_BT$, σ is the hard core diameter (identical to the bond length), $\lambda\sigma$ is the square well diameter ($1\leqslant\lambda\leqslant 2$), and $-\epsilon$ is the well depth (which is used to define a reduced temperature $T^*=1/\beta\epsilon$). In the limit of $\lambda\to 1$ or $\epsilon\to 0(T^*\to\infty)$ the model reduces to a tangent-hard-sphere polymer.

B. Monte Carlo methods

In order to test the accuracy of our BGY theory for polymer rings we have performed Monte Carlo (MC) simulations of square-well n-mer rings with $4\leqslant n\leqslant 200$ and $\lambda=1.5$ over a wide range of reduced temperatures T^*. Our MC algorithm involves two pivotlike moves, an axial rotation and a reflection, similar to the moves proposed by Madras *et al.* for ring polymers on a lattice.[29] For both moves two nonbonded ''pivot'' sites i and j are chosen at random ($1<|i-j|<n-1$) and the intervening ring segment is moved in such a way that the ring connectivity is maintained. We define the ''pivot axis'' as the line joining the centers of the two pivot

sites i and j and the ''pivot segment'' as the intervening ring segment $[i+1,\ldots,j-1]$ (where, for $j<i$, we use the cyclic labeling convention $i \equiv i+n$). For the axial rotation move the pivot segment is rigidly rotated by a randomly chosen angle $\alpha \in (0,2\pi)$ about the pivot axis while for the reflection move the pivot segment is reflected through the plane which forms the perpendicular bisector to the pivot axis. The pivot segment may be a single site for the axial rotation move (which corresponds to Baumgartner's MC move for hard-sphere rings[30]) while it must consist of at least two sites for the reflection move. In the simulation these two pivot moves are randomly attempted with equal probability. We note that this algorithm samples all possible ring configurations, including those containing knots.

To determine if an attempted move is to be accepted we first check for any hard-core overlaps in the trial configuration. If such an overlap exists the trial configuration is rejected and the old configuration is restored. If there are no hard-core overlaps we compute the energy E_{trial} of the trial configuration and compare it to the energy E of the old configuration. If $E_{\text{trial}}<E$, the move is accepted; otherwise we employ the Metropolis algorithm to determine acceptance.[31] That is we compare the ratio $\exp(-\beta E_{\text{trial}})/\exp(-\beta E)$ to a random number in the range $[0,1]$. If this ratio is greater than the random number the move is accepted; otherwise it is rejected. We assume that it takes at least n accepted moves to generate a statistically independent ring conformation.

The simulation consists of three phases; ring generation, equilibration, and data production. The initial ring configuration is generated by placing the centers of the n square-well sites at the vertices of an n-sided regular polygon in the $x-y$ plane. The ring is equilibrated for $N/10$ MC cycles where a single MC cycle consists of n attempted pivot moves. During the equilibration phase the acceptance fraction of attempted moves is determined. The production phase of the simulation consists of N MC cycles with data being accumulated every 1/(acceptance fraction) cycles. This data is collected in up to 10 blocks and block averaging is used to estimate errors in the final results.[31] In the simulations we compute a variety of site–site distribution functions and mean-square site–site separations, in addition to the mean-square radius of gyration, the average internal energy, and the specific heat. The latter quantity is determined using the fluctuation relation

$$C_v/k_B = \beta^2[\langle E^2\rangle - \langle E\rangle^2], \tag{7}$$

where the brackets $\langle\ \rangle$ denote an ensemble average. For the results presented here the lengths of the simulations were in the range $10^5 \leqslant N \leqslant 10^8$ MC cycles. In the case of a tangent-hard-sphere n-mer ring (i.e., $T^*\to\infty$) our MC algorithm gives results in agreement with those of Chen[32] and with the $n=4$ exact results given in the Appendix.

In order to compare the behavior of rings and chains we have also performed simulations on linear square-well n-mer chains with $4 \leqslant n \leqslant 200$ and $\lambda=1.5$. We use the standard pivot algorithm[33,34] in which a single pivot site $i\,(i\neq 1,n)$ is chosen at random and the chain segment $[i+1,n]$ is rigidly rotated, via an Euler rotation, about the pivot site. The initial chain configuration is generated using a dimerization algorithm.[33] In all other respects the chain simulations are essentially the same as the ring simulations. Our MC results for square-well n-mer chains are in very good agreement with those of Dautenhahn and Hall[34] and of Zhou *et al.*[11,12] and with Taylor's exact $n=4$ results.[35]

III. RESULTS FOR A SQUARE-WELL RING

A. Intramolecular distribution functions

The full set of site–site intramolecular distribution functions provides detailed information about the microscopic structure of an interaction-site polymer. However, since no single one of these functions provides an overall picture of the polymer structure we find it useful to consider an average over the complete set of distribution functions. For an n-mer ring we define the following average density distribution function

$$\rho^{\text{ring}}(r) = \sum_{j=3}^{n-1} w_{1j}^{\text{ring}}(r) \tag{8}$$

while the corresponding function for an n-mer chain is given by

$$\rho^{\text{chain}}(r) = \frac{1}{n} \sum_{|i-j|>1} w_{ij}^{\text{chain}}(r). \tag{9}$$

These distribution functions give the average density of sites about an arbitrarily chosen reference site (excluding those sites directly bonded to the reference site). We have computed such density distribution functions for square-well n-mer rings and chains using both the BGY theory and MC simulations. As with the individual site-site distribution functions, these average density functions are identically zero for $r<\sigma$ (due to the hard-core potential) and are discontinuous at the square-well boundary ($r=\lambda\sigma$) by a factor of $\exp(1/T^*)$. These average functions are also discontinuous at $r=2\sigma$, due to the discontinuity in the $w_{i,i\pm 2}(r)$ functions at $r=2\sigma$, and display a cusp at $r=3\sigma$, due to the nonzero slope of the $w_{i,i\pm 3}(r)$ functions at $r=3\sigma$.

In Fig. 1 we show these average distribution functions across a series of reduced temperatures for both a square-well ring and chain with $n=64$ and $\lambda=1.5$. The discontinuous behavior of these average functions at small integral units of the bond length, noted above, arises from bonding constraints and is similar for rings and chains at all temperatures. Beyond this complex local structure these density distribution functions display a single peak and smoothly fall off to zero. At the higher temperatures ($T^*\geqslant 3$) the ring and chain intramolecular density functions are quite distinct from each other as the ring functions drop to zero rather abruptly while the chain functions display a pronounced tail. The global collapse of both the ring and the chain is clearly evident from this series of distribution functions. With decreasing temperature (worsening solvent conditions) the location of the density peaks shift to smaller distances and the distribution functions narrow as the overall size of the polymers becomes more compact. In the low temperature (poor sol-

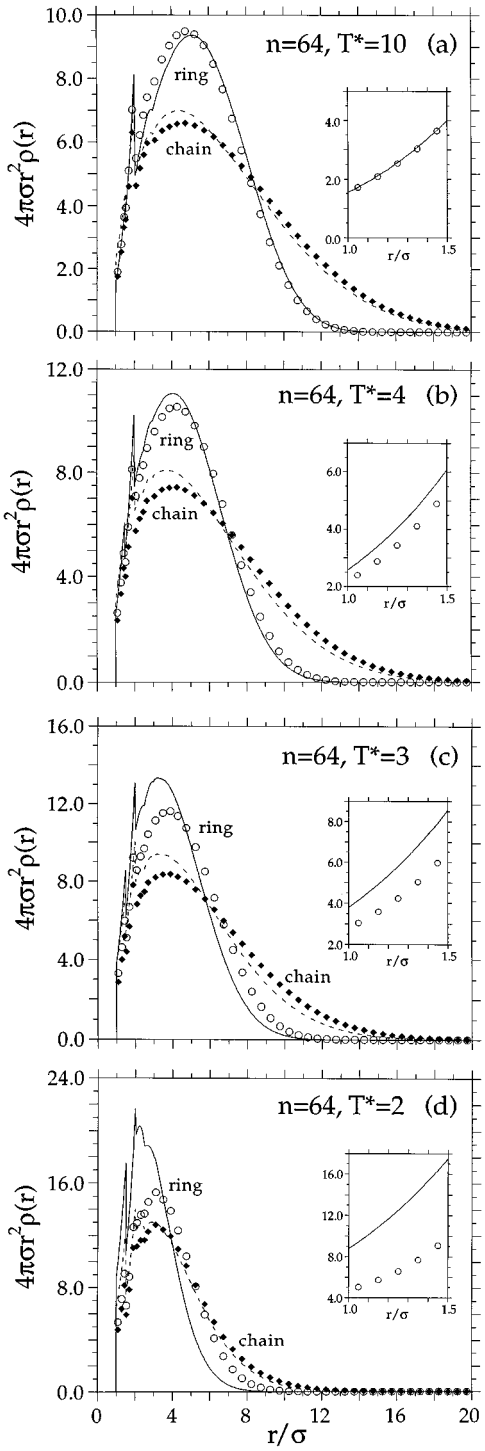

FIG. 1. Average intramolecular density distribution, $4\pi\sigma r^2\rho(r)$, for an isolated square-well 64-mer ring and chain with well diameter $\lambda=1.5$ at the reduced temperatures $T^*=10$ (a), 4 (b), 3 (c), and 2 (d). The solid and dashed lines are the BGY results for rings and chains, respectively, while the symbols (O, ◆) are the corresponding Monte Carlo results. The inset shows the same distribution function for the 64-mer ring in the range of the square-well potential ($\sigma<r<\lambda\sigma$).

vent) regime ($T^*\leqslant 2$) the ring and chain distribution functions become increasing similar and display well defined short-range structure characteristic of a dense fluid. At very low temperatures these distribution functions are nearly identical. For example, at $T^*=1$ (not shown) the MC data for the ring and chain are practically superimposable.

The BGY results for the average density distribution functions for both rings and chains are quite accurate at high temperatures ($T^*\geqslant 4$) and display qualitatively correct behavior for lower temperatures. In the low temperature regime the BGY theory tends to ''overcollapse'' both the ring and chain polymers as evidenced by distribution functions which are too narrow and shifted too far to the left in comparison with the MC results. As a result of this overcollapse the BGY theory will underestimate the average internal energy of the polymer which is determined by the magnitude of the distribution function within the range of the square well ($\sigma\leqslant r\leqslant\lambda\sigma$). The BGY results for the individual site–site ring distribution functions are found to obey the Eq. (1b) translational invariance condition reasonably well [e.g., the mean-square distance between pairs of sites $(1,\nu)$ and $(1,n-\nu+2)$ generally differ by only a few percent or less]. The quality of agreement between the BGY and MC results for the individual site–site ring and chain functions is comparable to that obtained for the average density functions shown in Fig. 1.

B. Average configurational and energetic properties

The average density distribution functions described above provide a concise overall view of the microscopic structure of an interaction-site polymer. These functions can also be used to compute a variety of average global properties of the polymer. For example, the mean-square radius of gyration of an n-mer ring or chain is related to the second moment of the average density distribution as follows:

$$\langle R_g^2\rangle=\frac{1}{n^2}\left\{a_n\sigma^2+\frac{n}{2}\int dr r^2[4\pi r^2\rho(r)]\right\}, \tag{10}$$

where a_n is the number of bonds in the n-mer (i.e., $a_n=n$ for a ring and $a_n=n-1$ for a chain).

In Fig. 2 we plot the mean-square radius of gyration $\langle R_g^2\rangle$ divided by n as a function of reduced temperature T^* for square-well n-mer rings with $8\leqslant n\leqslant 200$ and $\lambda=1.5$. In the high temperature limit ($T^*\geqslant 10$) the ring is in the expanded state and its configurational properties are essentially those of a tangent-hard-sphere ring (see Table I). With decreasing temperature the overall size of the ring, as measured by $\langle R_g^2\rangle$, is seen to decrease at first slowly and then more rapidly in the $4>T^*>1$ range. Below $T^*\approx 1$, $\langle R_g^2\rangle$ approaches an asymptotic low temperature limit. In comparison with the MC data, the overall shape of the BGY curves is correct (being nearly quantitative for $T^*>4$), although the theory slightly overestimates $\langle R_g^2\rangle$ at high temperatures and underestimates it at low temperatures. The sigmoidal shape of the $\langle R_g^2\rangle$ vs T^* curves is evidence of a ring collapse transition. As the rings get larger the fall-off in $\langle R_g^2\rangle$ becomes steeper indicating a sharpening collapse transition with increasing n. In the large n limit we expect such $\langle R_g^2\rangle/n$ curves to intersect at the theta temperature and thus the crossing of the $n=64$ and 200 curves in the vicinity of $T^*\approx 3$ gives an estimate of T_θ.

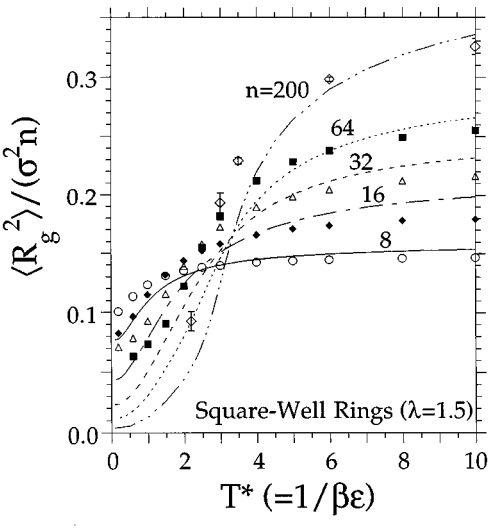

FIG. 2. Scaled mean-square radius of gyration $\langle R_g^2\rangle/n\sigma^2$ as a function of reduced temperature T^* for square-well n-mer rings ($8\leqslant n\leqslant 200$ as indicated) with well diameter $\lambda=1.5$. The solid and dashed lines are the results from the BGY theory while the symbols are the corresponding Monte Carlo results for $n=8$ (○), 16 (◆), 32 (△), 64 (■), and 200 (◇). The crossing of the $n=64$ and 200 curves in the vicinity of $T^*\approx 3$ approximately locates the theta temperature.

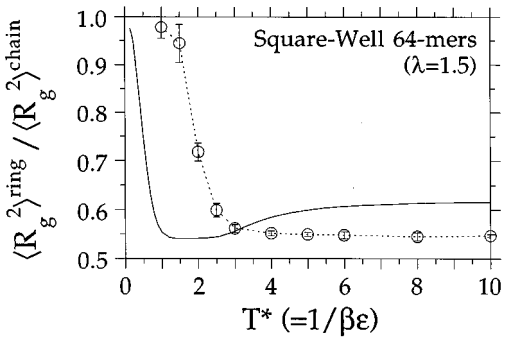

FIG. 3. Ratio of the ring to chain mean-square radius of gyration $\langle R_g^2\rangle$ as a function of reduced temperature T^* for square-well 64-mers with well diameter $\lambda=1.5$. The solid line is the BGY result and the symbols are the Monte Carlo results. (The dashed line is meant only as a guide for the eye.)

At high temperatures the radius of gyration of a ring polymer is expected to be much smaller than that of the corresponding chain (by a factor of 1/2 for ideal or Gaussian polymers[36]) while at low temperatures the density distribution functions shown in Fig. 1 indicate that the overall size of rings and chains becomes comparable. This behavior is seen more clearly in Fig. 3 where we plot the ratio of the radii of gyration, $g=\langle R_g^2\rangle^{\mathrm{ring}}/\langle R_g^2\rangle^{\mathrm{chain}}$, for square-well rings and chains with $n=64$ and $\lambda=1.5$ as a function of temperature. At high temperatures this ratio is seen to be slightly larger than the ideal value of $g=1/2$ ($g\approx 0.55$ MC, $g\approx 0.62$ BGY). With decreasing temperature this ratio remains fairly constant and then, at some low temperature, rises sharply to near unity. Assuming that rings and chains collapse to essentially the same final state, we can identify this sudden rise in g with the collapse transition and thus estimate the collapse transition temperature. From the BGY results we estimate $T^*_{\mathrm{collapse}} \lesssim 1.0$ while the MC data yield $1.0 \lesssim T^*_{\mathrm{collapse}} \lesssim 2.0$.

More definitive information about the location and nature of the collapse transition is provided by considering the energetic properties of the polymer ring. The average internal energy per site of an n-mer is given in terms of the average density distribution by

$$\langle E\rangle/n = \tfrac{1}{2}\int dr u(r)[4\pi r^2\rho(r)]. \tag{11}$$

For the square-well potential [Eq. (6)] the average energy depends only on the density distribution within the range of the well ($\sigma\leqslant r\leqslant\lambda\sigma$). In Fig. 4 we plot the average energy per site $\langle E\rangle/n\epsilon$ for square-well n-mer rings with $8\leqslant n\leqslant 64$ and $\lambda=1.5$ as a function of reduced temperature T^*. This average energy is fairly constant, though slowly decreasing, for $T^*>3$ and drops rapidly for $T^*<3$. The increase in $-\langle E\rangle$ reflects the decrease in $\langle R_g^2\rangle$ since the average number of square-well overlaps increases as the overall size of the ring polymer decreases. The BGY results for the average energy are quite accurate at higher temperatures but then greatly overestimate the increase in $-\langle E\rangle$ at lower temperatures. As discussed in our previous work on an isolated square-well

TABLE I. MC results for the radii of gyration for tangent-hard-sphere n-mer rings and chains (i.e., the $T^*\to\infty$ limit). The numbers in parentheses indicate the approximate error in the last digit shown.

n	$\langle R_g^2\rangle^{\mathrm{ring}}/\sigma^2$	$\langle R_g^2\rangle^{\mathrm{chain}}/\sigma^2$
8	1.194(1)	2.099(1)
16	3.000(3)	5.404(3)
32	7.39(1)	13.43(1)
50	13.02(1)	23.75(2)
64	17.73(1)	32.43(3)
100	30.8(1)	56.6(1)
200	71.8(2)	132.5(3)

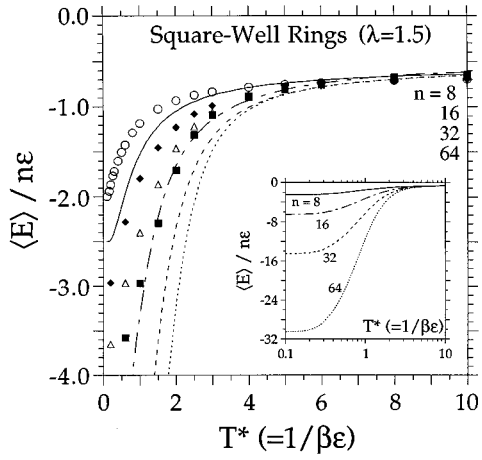

FIG. 4. Average energy per site $\langle E\rangle/n\epsilon$ as a function of reduced temperature T^* for square-well n-mer rings ($8\leqslant n\leqslant 64$ as indicated) with well diameter $\lambda=1.5$. The solid and dashed lines are the results from the BGY theory while the symbols are the corresponding Monte Carlo results for $n=8$ (○), 16 (◆), 32 (△), and 64 (■). The inset semilog plots show the asymptotic low temperature behavior of the BGY theory.

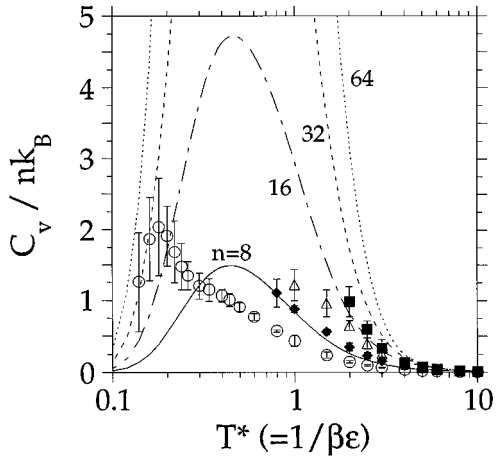

FIG. 5. Specific heat per site C_v/nk_B as a function of reduced temperature T^* for square-well n-mer rings ($8 \leqslant n \leqslant 64$ as indicated) with well diameter $\lambda=1.5$. The solid and dashed lines are the results from the BGY theory while the symbols are the corresponding Monte Carlo results for $n=8$ (○), 16 (♦), 32 (△), and 64 (■). The BGY curves all peak at $T^* \approx 0.45$.

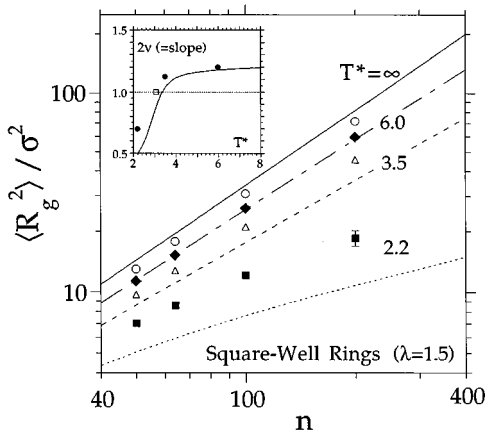

FIG. 6. Mean-square radius of gyration $\langle R_g^2 \rangle/\sigma^2$ vs ring size n for square-well rings with well diameter $\lambda=1.5$ for a range of reduced temperatures T^* as indicated. The solid and dashed lines are the results from the BGY theory while the symbols are Monte Carlo simulation results for $T^*=\infty$ (○), 6.0 (♦), 3.5 (△), and 2.2 (■). Inset: Scaling exponent 2ν (i.e., slope of above lines), determined from the BGY theory (—) and the above simulation data (●), vs T^*. The open square locates the Monte Carlo result for the theta temperature of a square-well chain with $\lambda=1.5$ (Ref. 37).

chain,[27] the quantity $|\langle E \rangle / n\epsilon|$ is simply half the number of square-well overlaps per site and thus, due to geometric constraints, should not exceed ~5. However, the BGY theory for rings gives a low temperature limit of $|\langle E \rangle / n\epsilon| = (n-3)/2$ which, for large n, violates this geometric restriction. Although quantitatively inaccurate at low temperatures, the sigmoidal shape of the BGY $\langle E \rangle / n\epsilon$ vs T^* curves is qualitatively correct and indicates that the polymer rings do indeed undergo a collapse transition.

The actual collapse transition temperature can be determined from the single ring specific heat which is given by the slope of these $\langle E \rangle / n\epsilon$ vs T^* curves [i.e., $C_v/nk_B = d(\langle E \rangle / n\epsilon)/dT^*$]. In Fig. 5 we plot this specific heat per site C_v/nk_B for square-well ring n-mers with $8 \leqslant n \leqslant 64$ and $\lambda=1.5$ as a function of reduced temperature. The BGY results for the specific heat give a smooth peak through the ring collapse with a maximum located at $T^*_{\text{collapse}} \approx 0.45$ for all values of n. In comparison with the Monte Carlo data, the actual magnitudes of the BGY specific heat results are clearly too large for $n \geqslant 16$ and $T^* < 3$ (as expected due to the overly steep BGY $\langle E \rangle / n\epsilon$ curves in Fig. 4). For the larger rings ($n \geqslant 16$) our Monte Carlo data for the specific heat are limited to $T^* \gtrsim 1$ and thus we only see the high-temperature tail of the C_v peaks and are unable to locate rigorously the actual collapse transition temperatures. For the isolated 8-mer ring we have performed additional Monte Carlo calculations in the neighborhood of the collapse transition. The 8-mer ring specific heat displays a broad peak in the range $0.1 < T^* < 2.0$ with a shoulder at $T^* \approx 0.35$, roughly coincident with the peak in the BGY results, and a low temperature maximum at $T^* \approx 0.2$. Similar complex specific heat curves have been previously observed by Zhou *et al.* for square-well chains.[11,12] After detailed study, these authors have shown that the high temperature shoulder can be associated with a condensationlike collapse transition and the low temperature peak marks a liquid–solid-like ordering transition. We suspect that the same interpretation applies to our square-well ring MC results.

C. Flory exponent and theta temperatures

Both our BGY and Monte Carlo results demonstrate that a square-well ring polymer undergoes a transition from an expanded to a collapsed state with decreasing temperature. Experimentally, the expanded and collapsed states are associated with so called good and poor solvent conditions, respectively.[1,2] These two states can be distinguished by examining the scaling exponent 2ν, which relates the n-mer ring radius of gyration to polymerization index n via the scaling relationship $\langle R_g^2 \rangle \sim n^{2\nu}$. The expanded state (good solvent regime) is associated with a scaling exponent of $2\nu > 1$ while in the collapsed state (poor solvent regime) $2\nu < 1$. The intermediate case of $2\nu = 1$ defines the so-called theta or ideal state in which the scaling behavior of the ring polymer is identical to that of a Gaussian ring.

This scaling relationship is verified in Fig. 6, where we show a log–log plot of the square-well n-mer ring radius of gyration vs n for a range of temperatures. Comparing the BGY and MC results in this plot, the BGY theory is seen to somewhat overestimate the ring size for $T^* > 6$ and underestimate it for $T^* < 6$. However, the scaling behavior (i.e., the slopes of the lines) of the BGY and MC results is quite similar. In the high temperature ($T^* \to \infty$) limit the BGY results for $40 \leqslant n \leqslant 400$ give a scaling exponent of $2\nu = 1.27$ while the Monte Carlo data for $50 \leqslant n \leqslant 200$ give an exponent of $2\nu = 1.23$. The fact that these exponents exceed the expected Flory value of 6/5 indicates that the ring sizes considered here are not large enough to be in the asymptotic scaling regime. With decreasing temperature the scaling exponent 2ν decreases and, as seen in the Fig. 6 inset, passes through unity at $T^* = T^*_\theta \approx 3.4$. For low temperatures ($T < T_\theta$) the

TABLE II. BGY results for the theta temperatures T_θ^* of square-well rings and chains with well diameter $\lambda\sigma$. The numbers in parentheses are estimates of the uncertainty in the last digit shown.

λ	Ring	Chain
1.25	1.50(5)	1.45(5)
1.50	3.4(1)	3.2(1)
1.75	6.5(1)	6.0(1)
2.00	11.6(2)	10.6(2)

scaling exponent should approach a limiting value of 2/3.[2] However, due to the over-collapse of the rings in the BGY theory, the low temperature BGY exponent falls below this limiting value. While the above results focus on rings with well width $\lambda=1.5$, we have also used our BGY theory to compute theta temperatures for square-well rings with well widths other than $\lambda=1.5$ and these are given in Table II.

IV. DISCUSSION

In this work we have presented a Born–Green–Yvon integral equation theory for an isolated interaction-site ring polymer. This theory has been used to make a detailed study of the configurational and energetic properties of square-well n-mer rings with $4\leqslant n\leqslant 400$ and $\lambda=1.5$ over a wide range of temperatures. In the high temperature limit the square-well ring is identical to the tangent-hard-sphere ring (i.e., the ''pearl necklace'' model). With decreasing temperature both the average size and internal energy of the ring decrease and a collapse transition is signaled by a peak in the single ring specific heat at $T^*\approx 0.45$, independent of the ring size n. For large n the mean-square radius of gyration obeys the scaling relationship $\langle R_g^2\rangle \sim n^{2\nu}$ and in the high temperature limit the BGY theory gives a scaling exponent of $2\nu=1.27$. As the temperature is decreased the scaling exponent also decreases passing through unity at a theta temperature of $T_\theta^* \approx 3.4$.

In order to assess the accuracy of our BGY theory we have also performed Monte Carlo simulations of square-well ring polymers with $4\leqslant n\leqslant 200$ and $\lambda=1.5$. In comparison with the MC data for the average density distribution, mean-square radius of gyration, and average internal energy the BGY theory for rings yields results which are nearly quantitative (generally within $\sim$10%) for $T>T_\theta$ and are qualitatively correct for $T<T_\theta$. In the limit of very low temperatures the BGY theory tends to overcollapse the ring polymers. The MC specific heat data indicates that the 8-mer ring collapses at a transition temperature of $T^*_{\text{collapse}}\approx 0.35$ in fair agreement with the BGY result of $T^*_{\text{collapse}}\approx 0.45$. However, the complex structure of the MC specific heat curves, seen here for 8-mer rings and by Zhou *et al.* for square-well chains,[11,12] is not reproduced by the integral equation theory. For rings larger than $n=8$ our MC specific heat data is insufficient to locate a collapse temperature. However, from our MC data for the ring to chain size ratio g (Fig. 3) we estimate $1.0\lesssim T^*_{\text{collapse}}\lesssim 2.0$ for square-well 64-mers with $\lambda=1.5$. This estimate agrees with the collapse temperature $T^*_{\text{collapse}}\approx 1.5$ reported by Zhou *et al.* for a square-well 64-mer chain[12] which, in turn, supports the idea that rings and chains do have a common T_{collapse}. Finally, the MC results give a high temperature scaling exponent of $2\nu=1.23$ which is very similar to the BGY result and suggests that the rings studied here are too small to be in the asymptotic scaling regime (where we expect $2\nu\approx 6/5$).

It is interesting to compare the BGY and MC results obtained here for square-well rings to the corresponding results for square-well chains. We make such a comparison in Fig. 1, for the average site density distribution functions, and in Fig. 3, for the average size ratio, for 64-mer rings and chains. Both the BGY and MC results demonstrate that at high temperatures (good solvent) rings are much more compact than chains while with decreasing temperature (worsening solvent) the microscopic structure of rings and chains becomes increasingly similar. The average size of a ring, as measured by the mean-square radius of gyration, is slightly more than 1/2 that of a chain at high temperatures while in the low temperature, collapsed, state rings and chains have essentially the same size. In the limit of large n and $T^*\rightarrow\infty$ (good solvent) our MC results, given in Table I, suggest that the ring to chain size ratio approaches a value of $g\approx 0.54$. This asymptotic value of g agrees with a variety of other simulation results[13,38,39] and is consistent with the present BGY results, renormalization group calculations,[40] and experimental measurements.[41,42] The scaling of $\langle R_g^2\rangle$ with n is found to be very similar for rings and chains. In the high temperature limit the BGY theory gives a Flory exponent of $2\nu=1.27$ for rings and 1.31 for chains while the MC calculations yield $2\nu=1.23$ for rings and 1.24 for chains. The temperature dependence of the scaling exponent 2ν has been used to locate the theta temperature for both rings and chains. The BGY values of T_θ for square-well rings are very similar to, although slightly larger than, the corresponding T_θ values for square-well chains (Table II). We have shown previously that these BGY T_θ values for chains are in good agreement with MC results.[27] Experimentally it is found, using the criterion of a vanishing second virial coefficient, that T_θ^{ring} is slightly less than T_θ^{chain} (contrary to our results).[43–45] However, Garcia Bernal *et al.* and others suggest that for ring polymers, T_θ should not be defined in this manner but rather, should be defined through the ideal scaling of the polymer configurational properties (as is done here).[38,39] Using this latter definition, the experimental theta temperatures for rings and chains are found to be nearly the same. Finally, our BGY specific heat results indicate that rings and chains collapse at nearly the same temperature in agreement with the lattice results of Tesi *et al.*[13] The BGY theory yields a value of $T^*_{\text{collapse}}\approx 0.45$ for square-well rings and 0.40 for square-well chains with $\lambda=1.5$, independent of size n. This collapse transition temperature is correct for small rings and chains (i.e., $n=8$) but should increase with increasing n, approaching T_θ in the limit of large n. We note that such limiting behavior is suggested in Fig. 2 by the steepening of the $\langle R_g^2\rangle$ vs T^* curves with increasing n in the vicinity of T_θ.

In conclusion, our BGY theory for an isolated ring polymer yields results of comparable quality to those given by our previously presented BGY theory for isolated chains. The ring theory is based on a three-site superposition ap-

proximation and requires as input the site–site intramolecular distribution functions for a single chain. Here we use the superposition approximation previously employed in our single chain BGY theory[27] and we use the results of the latter as input into the ring theory. The success of the present theory for rings lends additional support to the validity of the Eq. (4) superposition approximation. This approximation could be tested further by using MC results for the single chain functions as input into the ring theory [Eq. (5)]. However, since our current goal has been to develop a self-contained BGY theory for rings we have not pursued such calculations. Finally, it may be possible to generalize the BGY approach used here to study polymers of other topologies.

ACKNOWLEDGMENTS

Financial support from the National Science Foundation (Grant No. DMR-9424086) and the Dreyfus Foundation is gratefully acknowledged. J.L.M. thanks the NSF-REU program for their support.

APPENDIX: EXACT RESULTS FOR THE TANGENT-HARD-SPHERE 4-MER RING

The three-site distribution function for a flexible tangent-hard-sphere chain of length $n=4$ can be written exactly as

$$w_{134}^{\text{chain}} = w_{13}^{\text{chain}} w_{34}^{\text{chain}} \frac{Z_3^{\text{chain}}}{Z_4^{\text{chain}}} \left[1 - \frac{1}{\pi}\, \phi(r_{14}, r_{13}, \lambda = 1) \right] \qquad \sigma \leqslant r_{14} \leqslant 3\sigma, \tag{A1}$$

where w_{13}^{chain} is the end-to-end distribution function for a 3-mer chain, $w_{34}^{\text{chain}}(r) = s(r)$, Z_n^{chain} is the partition function for an isolated n-mer chain, and the function ϕ is given by Eq. (33) of Ref. 35. Substituting Eq. (A1) into Eq. (2) yields the following exact expression for the 4-mer ring two-site distribution function:

$$w_{13}^{\text{ring}}(x) = \frac{1}{4\pi\sigma^3 N x^2} \cos^{-1}(4 - x^2)^{-1/2} \qquad 1 \leqslant x \leqslant 3^{1/2}, \tag{A2}$$

where $x = r/\sigma$ and the normalization constant is $N = 2\pi Z_4^{\text{ring}} = 2\pi - 6\tan^{-1}(2^{1/2})$. The mean-square distance between sites 1 and 3 is $\langle r_{13}^2 \rangle / \sigma^2 = [16\pi - 2^{1/2} - 45\tan^{-1}(2^{1/2})]/6N$ and the radius of gyration is $\langle R_g^2 \rangle = \sigma^2/4 + \langle r_{13}^2 \rangle / 8 \approx 0.471\,53\sigma^2$.

[1] P. J. Flory, *Principles of Polymer Chemistry* (Cornell University Press, Ithaca, 1953).
[2] A. Yu. Grosberg and A. R. Khokhlov, *Statistical Physics of Macromolecules* (AIP, New York, 1994).
[3] A. Baumgartner, J. Chem. Phys. **72**, 871 (1980).
[4] I. Webman, J. L. Lebowitz, and M. H. Kalos, Macromolecules **14**, 1495 (1981).
[5] M. Bishop and J. P. J. Michels, J. Chem. Phys. **84**, 447 (1986).
[6] N. Karasawa and W. A. Goddard III, J. Phys. Chem. **92**, 5828 (1988).
[7] A. Milchev, W. Paul, and K. Binder, J. Chem. Phys. **99**, 4786 (1993).
[8] G. Tanaka and W. L. Mattice, Macromolecules **28**, 1049 (1995).
[9] J. Ma, J. E. Straub, and E. I. Shakhnovich, J. Chem. Phys. **103**, 2615 (1995).
[10] M. Wittkop, S. Kreitmeier, and D. Goritz, J. Chem. Phys. **104**, 3373 (1996); this article contains an extensive set of references regarding the collapse transition.
[11] Y. Zhou, M. Karplus, J. M. Wichert, and C. K. Hall (unpublished).
[12] Y. Zhou, C. K. Hall, and M. Karplus, Phys. Rev. Lett. **77**, 2822 (1996).
[13] M. C. Tesi, E. J. Janse van Rensburg, E. Orlandini, and S. G. Wittington, J. Phys. A **29**, 2451 (1996).
[14] I. Nishio, S.-T. Sun, G. Swislow, and T. Tanaka, Nature **281**, 208 (1979).
[15] S.-T. Sun, I. Nishio, G. Swislow, and T. Tanaka, J. Chem. Phys. **73**, 5971 (1980).
[16] P. Stepanek, C. Konak, and B. Sedlacek, Macromolecules **15**, 1214 (1982).
[17] P. Vidakovic and F. Rondelez, Macromolecules **17**, 418 (1984).
[18] I. H. Park, Q.-W. Wang, and B. Chu, Macromolecules **20**, 1965 (1987).
[19] B. Chu, I. H. Park, Q.-W. Wang, and C. Wu, Macromolecules **20**, 2833 (1987).
[20] K. Kubota, S. Fujishige, and I. Ando, J. Phys. Chem. **94**, 5154 (1990).
[21] M. Nakata, Phys. Rev. E **51**, 5770 (1995).
[22] C. Wu and S. Zhou, Phys. Rev. Lett. **77**, 3053 (1996).
[23] J. Naghizadeh, J. Chem. Phys. **48**, 1961 (1968); J. Naghizadeh and N. K. Ailawadi, *ibid.* **63**, 650, 657 (1975).
[24] J. G. Curro, P. J. Blatz, and C. J. Pings, J. Chem. Phys. **50**, 2199 (1969).
[25] B. C. Eu and H. H. Gan, J. Chem. Phys. **99**, 4084 (1993); H. H. Gan and B. C. Eu, *ibid.* **99**, 4103 (1993); **100**, 5922 (1994).
[26] P. Attard, J. Chem. Phys. **102**, 5411 (1995).
[27] M. P. Taylor and J. E. G. Lipson, J. Chem. Phys. **104**, 4835 (1996).
[28] S. G. Whittington and L. G. Dunfield, J. Phys. A **6**, 484 (1973).
[29] N. Madras, A. Orlitsky, and L. A. Shepp, J. Stat. Phys. **58**, 159 (1990).
[30] A. Baumgartner, J. Chem. Phys. **76**, 4275 (1982).
[31] M. P. Allen and D. J. Tildesley, *Computer Simulation of Liquids* (Oxford University Press, Oxford, 1987).
[32] Y. Chen, J. Chem. Phys. **75**, 5160 (1981). As noted in Ref. 38, the algorithm used in this work yields a slightly biased distribution of ring conformations.
[33] A. D. Sokal, in *Monte Carlo and Molecular Dynamics Simulations in Polymer Science*, edited by K. Binder (Oxford University Press, Oxford, 1995), Chap. 2.
[34] J. Dautenhahn and C. K. Hall, Macromolecules **27**, 5399 (1994).
[35] M. P. Taylor, Mol. Phys. **86**, 73 (1995).
[36] B. H. Zimm and W. H. Stockmayer, J. Chem. Phys. **17**, 1301 (1949).
[37] J. M. Wichert and C. K. Hall, Macromolecules **27**, 2744 (1994).
[38] J. M. Garcia Bernal, M. M. Tirado, J. J. Freire, and J. Garcia de la Torre, Macromolecules **23**, 3357 (1990); **24**, 593 (1991).
[39] A. M. Rubio, J. J. Freire, M. Bishop, and J. H. R. Clarke, Macromolecules **28**, 2240 (1995).
[40] J. F. Douglas and K. F. Freed, Macromolecules **17**, 2344 (1984).
[41] J. S. Higgins, K. Dodgson, and J. A. Semlyen, Polymer **20**, 553 (1979).
[42] M. Ragnetti, D. Geiser, H. Hocker, and R. C. Oberthur, Makromol. Chem. **186**, 1701 (1985).
[43] J. Roovers and P. M. Toporowski, Macromolecules **16**, 843 (1983); J. Roovers, J. Polym. Sci. Polym. Phys. Ed. **23**, 1117 (1985).
[44] G. Hild, C. Strazielle and P. Rempp, Eur. Polym. J. **19**, 721 (1983).
[45] P. Lutz, G. B. McKenna, P. Rempp, and C. Strazielle, Makromol. Chem. Rapid Commun. **7**, 599 (1986).